SLAC – PUB – 3473
October 1984
A

New Radiofrequency Technique for Deposition of Hard Carbon Films*

A.R. NYAIESH, R.E. KIRBY, F.K. KING, AND E.L. GARWIN

Stanford Linear Accelerator Center
Stanford University, Stanford, California, 94305

ABSTRACT

We have developed a new technique to produce diamond-like carbon films in an rf system with water cooled electrodes. Hydrocarbon gas is leaked into the experimental chamber through the upper electrode which is a pyrex cylinder inside a coil forming an rf oven. The gas (CH_4) undergoes ionization/dissociation in one rf field, within an axial magnetic field. A circular water cooled electrode supports the substrate to be coated, and is powered from a second rf generator, developing a negative self bias on the substrate. Thus dissociation and ion production at the upper electrode and ion acceleration by the lower electrode could be separately controlled to optimize the film properties. It is shown that low stress, highly dense carbon films can be deposited by this method. Information is also given on bulk and surface properties as well as modification of these properties by the deposition conditions.

Presented at the 31st National Symposium of the
American Vacuum Society, Reno, Nevada, December 3-7, 1984

* Work supported by the Department of Energy, contract DE – AC03 – 76SF00515.

1. Introduction

Hard, insulating, optically transparent carbon films have various applications in the metallurgy, surface finishing, semiconductor and optical industries.[1-9] Their physical properties are extreme hardness (up to 6000 Kg/mm^2 Vickers hardness)[10], low coefficient of friction (μ = 0.04-0.08 coated steel vs. steel) [1,11], corrosion resistance and chemical inertness[2,5,12], high resistivity, on the order of $10^{12}\Omega$ -cm and, with infrared refractive index of about 2, have served as AR coatings on Si and Ge optical elements.

Various deposition techniques have been reported for hard carbon films which involve film growth under ion bombardment. This causes radiation damage of the carbon structure and hence yields an amorphous metastable phase of carbon. Chiefly, carbon films have been deposited by ion beam deposition from a C^+ ion source[13], dual Ar^+ ion beam sputtering from a carbon target[14], and dc[15] and rf[16] plasma decomposition of hydrocarbon monomer. Due to the resulting high film resistivity, the rf technique developed by Holland[16] is widely used. In this technique the film substrate does not have to be a conductor; positive surface charging on high resistivity carbon film (called a-C:H films here) is avoided by the flow of electrons from the plasma during the positive part of the rf cycle. Moreover the rf method has a higher current density than the ion beam deposition technique. The positive ion current bombarding the growing film can also be designed to make a uniform current density and thus a uniform film growth over a large area.

In this paper we describe a new method of a-C:H deposition in which an enhanced rf ionization of hydrocarbon monomer is utilized. The ionized species of monomer produced in an rf oven are accelerated towards a second rf electrode which carries the substrate and deposits a-C:H upon impact on the substrate. It appears that energetic ions sputter-etch the weakly bonded species in the carbon film structure, reducing the film stress and produce a highly dense a-C:H film. In this study, information is given on the bulk film properties as well

as modification of these properties by alteration of the deposition conditions. The surface properties of the films were investigated using Auger (AES), x-ray photoelectron (XPS) and secondary ion mass (SIMS) spectroscopy as well as by measuring the secondary electron emission (SEE) yield.

2. Experiment

2.1 Deposition apparatus and procedures

The deposition apparatus is shown in Fig. (1). It consists of a pyrex cylinder 15cm diameter x 30 cm high evacuated by a diffusion pump (750 ℓ/sec) backed by a mechanical pump and throttling gate valve. The chamber is evacuated to a base pressure of 1 x 10^{-7} torr (1.3 x 10^{-5} Pa) and, for deposition experiments, the throttle valve was adjusted so as to maintain a substantial gas flow. High purity CH_4 gas (99.99%) was leaked into the system through a needle valve via the upper electrode.

The upper electrode is a pyrex beaker of 6 cm diameter, inside an rf coil powered from a 2MHz rf generator, forming an rf oven. Very intense plasma is produced in this electrode and ionization is enhanced by an axial magnetic field which contains the plasma in the cylindrical volume between the two rf electrodes.

The planar, water-cooled-copper lower electrode is 6 cm. in diameter, coupled to an rf generator via a power meter and an impedance-matching π-network. The rf voltage is applied between ground and this electrode while the latter is allowed to assume a negative dc bias voltage determined by the deposition parameters (Table 1). The forward and reflected power to the substrate holder were measured with a wattmeter (Bird Model 43). The reflected power was kept at a negligible level by adjusting the π-network. The temperature of the growing film was measured by a pyrometer focused at the surface of the substrate holder at the center of the substrate carrier. The pyrometer band pass is 1.7 – 2.7

microns and is not disturbed by the optical emission of the plasma. The plasma intensity and the negative dc self bias of the substrate carrier can be controlled by independently changing the powers to the lower electrode and the rf oven, as well as by changing the axial magnetic field. The plasma is almost completely confined by the magnetic field to the volume between the two electrodes at the center of the chamber. Therefore the interaction between the plasma and its surroundings is minimized and this reduces the contamination from the chamber walls. Also, particles (eg. soot, dust, etc.) in contact with the plasma, like any floating probe, charge up negatively and are thus repelled from the negatively biased substrate, thereby aiding production of pinhole-free films.

2.2 SURFACE ANALYSIS SYSTEM

For surface studies, a-C:H is deposited on type 304 stainless steel substrates which have been mechanically polished with 5μm diamond paste and chemically cleaned. a-C:H samples prepared in the above manner are removed from the deposition apparatus and transferred to an ultrahigh vacuum (P ¡ 3×10^{-10}torr) system. The surface techniques available in this system are Auger (AES) and x-ray photoelectron spectroscopy (XPS), secondary ion mass spectrometry (SIMS) and measurement of the total secondary electron emission yield (SEE). In situ heating of the samples during analysis is also available. System control and data acquisition is under computer control (LSI 11/23 microcomputer). All results are stored in memory for subsequent processing and analysis.

SEE measurements are done via the retarding potential method[17] utilizing low probe currents (2nA). The AES electron beam is 50nA, rastered to give a current density of 2 $\times 10^{-3} A/m^{-2}$ which minimizes electron beam damage to the samples. Binding energy references for XPS are the palladium Fermi edge (BE = 0) and the silver $3d_{5/2}$ core line (BE = 368.2eV). The x-ray anode used was magnesium $K\alpha_{1,2}(h\nu = 1253.6\text{eV})$.

3. Results

3.1 GENERAL FILM EVALUATION

Films deposited at low operating pressures of 3-50 mtorr by the above technique show a grayish pale color, are transparent in IR and have no absorption band in visible and near UV (900 – 200nm). No quantitative stress measurements were carried out, but thick films of up to 10μm grown on thin glass, Si, Ge and plastics had neither adhesion failure nor bowing, as seen by observing the surface reflection of a linear light source. This result led us to believe that the films have low internal stress. The densities of these films were between 2.20 – 2.70, averaging 2.26 g cm^{-3}. However a-C:H films prepared at 80 – 200 mtorr pressure show a yellow transmission color, high compressive stress, and IR transparency, and exhibit absorption at 900 – 200nm wavelength in the visible and near UV. The densities of these films were between 1.85 – 2.10, averaging 1.95 g cm^{-3}. Both groups exhibit high electrical resistivity of $\sim 10^{12}\Omega$-cm, are hard, scratch resistant and insoluble in various solvents (i.e. concentrated HCl,HNO_3 and NaOH). We report here on two types of films produced in the 3 – 50 mtorr pressure range (referred to as #1 and #2). The deposition conditions for both #1 and #2 were: 200 watts power to substrate holder, 0.02 T axial magnetic field at the center of the pyrex cylinder and 5 mtorr pressure of CH_4. The negative self bias developed on the substrate was 1250 volts for #2 when the power to the rf oven was ~30 watts. The power to the rf oven was then increased which reduced the negative self bias on the substrate from 1250 volts to 500 volts for #1. Increasing the power to the rf oven is thought to aid gas phase reaction and polymerization on the oven walls and thereby reduces the film deposition rate on the substrate.

The film thicknesses were measured with AT-cut quartz crystals. Problems we encountered in film thickness measurements using quartz crystals are thought to be due to the kinetics of a-C:H growth from a C_nH_n plasma. The ionized cracking products produced in the rf oven are contained by the axial magnetic

field and accelerated towards the substrate surface. These carbon fragments will sputter-etch the substrate surface and cause the removal of some substrate material before the substrate is completely covered by the growing carbon film. This is similar to bias sputtering where the substrate is deposited and etched simultaneously. The film thicknesses quoted here are derived from the quartz crystal which was pre-coated with carbon to reduce this re-sputter effect.

The surface analysis samples were on stainless steel and the resistivity measurements utilized Al_2O_3 substrates. Our best estimates for the actual film thicknesses of the surface analysis samples are 35 – 75 nm for #1 and 390 nm for #2, respectively. The sheet resistance shows a mild dependency on the bias voltage from 100-1100 volts (as shown in Fig. (2)) but at lower than 100 volts rises by up to two orders of magnitude.

3.2 Surface Physics

Results are presented here for two representative types of films. One of these (#1 in Figures 3,4,5) appears to be a rather low density film, rich in hydrocarbons while the other (#2 in Figures 3 and 4) is suggestive of a more graphite (or diamond)-like composition. The SEE yield of argon sputter-cleaned bulk graphite and its XPS core level line is included for comparison.

Under analysis by SIMS, the sputter rate was considerably higher for #1 than #2. Hydrocarbon groups were present in the SIMS spectra thru the bulk of #1 as it was sputtered away. Since bulk carbon has a very low sputter rate, these results suggest that #1 was rich in polymerized hydrocarbons. A thin hydrocarbon layer was also present on the surface of #2. This is discussed further in the next section. The SIMS hydrogen (AMU 1) signal was rather constant in #1 but declined steadily (Figure 6) in #2. Other than the carbon and hydrogen signals, SIMS showed the usual presence of alkalis.

The SEE (Figure 3) results support the above thesis in that film #1 shows a high yield typical of surfaces covered by adventitous (adsorbed hydrocarbon)

carbon layers while #2 is more typical of graphite, both in peak yield and curve shape. The slope at higher energy in #1 suggests that the electron beam may be penetrating the low thickness film and producing backscattered electrons from the stainless substrate, thereby enhancing the yield at high incident energy.

The XPS core level results show a very graphite- or diamond- like structure (see discussion section) for film#2 while the core level for #1 is shifted to higher binding energy. The #1 core line also features a prominent shoulder which is extracted in the peak synthesis curve fit of Figure 5. The AES results indicate that the surfaces of both films contain some oxygen (#1 considerably more than #2) which was presumably picked up from water vapor during transfer from the deposition apparatus to the surface analysis system. #1 also showed evidence of the substrate (Fe, Ni, Cr) in both the XPS and AES confirming our SEE results that, indeed, #1 was quite thin.

4. Discussion

Film #2 is typical of a-C:H layers produced at 1250V substrate bias by the method described in the **Experiment** section. Type #2 films seem to be also covered by a very thin, low mass hydrocarbon which was detected by SIMS (by the presence of C_nH_n groups) and vanished very quickly. This thin layer is almost certainly produced in the deposition chamber rather than during transfer to the surface analysis chamber as determined by comparison to SIMS results for graphite and stainless steel substrates similarly exposed to room air. Craig and Harding[18] have found evidence for the existence of long-chain hydrocarbon in their a-C:H films from mass spectroscopy of film outgassing products. Figure 6 shows that there is also some hydrogen present in the bulk of films of type #2. However it is not clear how these fragments are bonded in the film since the hydrogen does not appear very IR active in the transmission range 200 – 4000 cm^{-1}, as determined by absorption measurements on Si substrates.

The binding energy of type#2 a-C:H films were compared to those of graphite (Figure 4) and diamond. The results of Pate et al[19] show a binding energy of 284.8eV for the 1×1 low energy electron diffraction (LEED) structure of the hydrogen-terminated surface of diamond (111) (graphite binding energy reference of 284.7eV). Liu et al[20] have a similar value of 284.6eV for rf plasma-deposited carbon films (no energy reference given). The results of Mori and Namba[21], however, give a much higher binding energy for both diamond and "diamondlike" carbon films of ~287eV with a somewhat low value for graphite of 283.8eV.

For films of type #2, our binding energies for the C1s core levels were in the range from 284.1 to 284.7eV (five samples). The curve fit of #1 in Figure 5 suggests that the main peak at 285.1eV is a hydrocarbon type structure with the small shoulder being an oxidized surface fraction. No shoulders of this type were observed on type #2 films.

5. Conclusion

Dense, insulating a-C:H films grown by a new method have been examined with various bulk and surface techniques, the results of which have been presented here. Films of both low and high secondary yield can be produced by varying the oven power (and thereby the substrate bias). A reduced negative substrate bias appears to produce films having a hydrocarbon-like structure. Increased substrate bias produces films whose surface properties are similar to graphite (and hydrogen-terminated diamond) and are in agreement with the XPS core level results of a previous study[20].

Table I

Deposition Parameters

R.F. Power	Upper electrode	20-500 (watt)
	Lower electrode (substrate carrier)	20 – 300 (watt)
R.F. Frequency		2(MHz)
Negative Self Bias (lower electrode)		50 – 1250 (volt)
Axial Magnetic Field		0.002 – 0.03(T)
Operating Pressure		2 – 200 (mtorr)
Deposition temperature during film growth		40 – 190°C
Substrate		304SS, glass, Si, Ge, Al_2O_3, plastics
Deposition rate		10 – 200 nm min^{-1}

Figure Captions

1. Dual rf powered electrode plasma system developed for growing a-C:H films.
2. Room temperature (R.T.) sheet resistance of as-deposited a-C:H films as a function of negative self-bias on the substrate.
3. Total secondary electron emission yield of two types of a-C:H films as a function of incident electron energy. The curve for bulk graphite is also shown.
4. C1s XPS binding energy of two types of a-C:H films and bulk graphite.
5. Peak synthesis curve fit of #1 C1s line of Figure 4 with hydrocarbon peak at 285.1 (—) and oxidized surface fraction at 286.8 (-.-.-.).
6. Integrated area of SIMS hydrogen (AMU 1) signal from sample type #2 as a function of sputtering time.

References

1. H. Dimigen and H. Hübsch, Philips Tech. Rev. 41, 186, (1983/84).
2. J. Zelez, RCA Rev. 43, 665 (1982).
3. B. Meyerson and F.W. Smith, J. Noncrystall. Solids 35-36, 435 (1980).
4. A. Bubenzer, B. Dischler and A.R. Nyaiesh, 13th Intl. Symp. on "Laser Damage in Optical Materials", Boulder, Colo., 1981, NBS Special Publication.
5. A. Bubenzer, B. Dischler and A.R. Nyaiesh, Thin Solid Films 91, 81 (1982).
6. L. Holland and S.M. Ojha, Thin Solid Films 48, L21 (1978).
7. L. Holland and S.M. Ojha, Thin Solid Films 58, 107 (1979).
8. D.R. McKenzie and L.M. Briggs, Solar Energy Mater. 6, 97 (1981).

9. N. Hosokawa, A. Konishi, H. Hiratsuka and K. Annoh, Thin Solid Films 73, 115 (1980).

10. T. Mori and Y. Namba, J. Vac. Sci. Techol. A 1(1), 23 (1983).

11. C.H.R. Weissmantel, Proc. IX IVC - V ICSS, Madrid, 299 (1983).

12. L. Holland and S.M. Ojha, Thin Solid Films 38, L17 (1976).

13. S. Aisenberg and R. Chabot, J. Appl. Phys. 42, 2953 (1971).

14. C.H.R. Weissmantel, Thin Solid Films 58, 255 (1976).

15. D.S. Whitmell and R. Willamson, Thin Solid Films 35, 255 (1976).

16. L. Holland, UK Patent 1582231, (App. Aug. 1976).

17. V.E. Henrich, Rev. Sci. Instrum. 45, 861 (1974).

18. S. Craig and G.L. Harding, J. Vac. Sci. Technol. 21, 83 and the references therein (1982).

19. B. Pate, M. Oshima, J. Silberman, A. Rossi, I. Lindau and W.E. Spicer, J. Vac. Sci. Technol A2(2), 957 (1984).

20. D. Liu, R. Dillon and J.A. Woollam, 16th Biennial Conference on Carbon, Amer. Carbon Soc., July 18-22, 1983, UC San Diego, CA, p.293.

21. T. Mori and Y. Namba, J. Appl. Phys. 55, 3276 (1984).

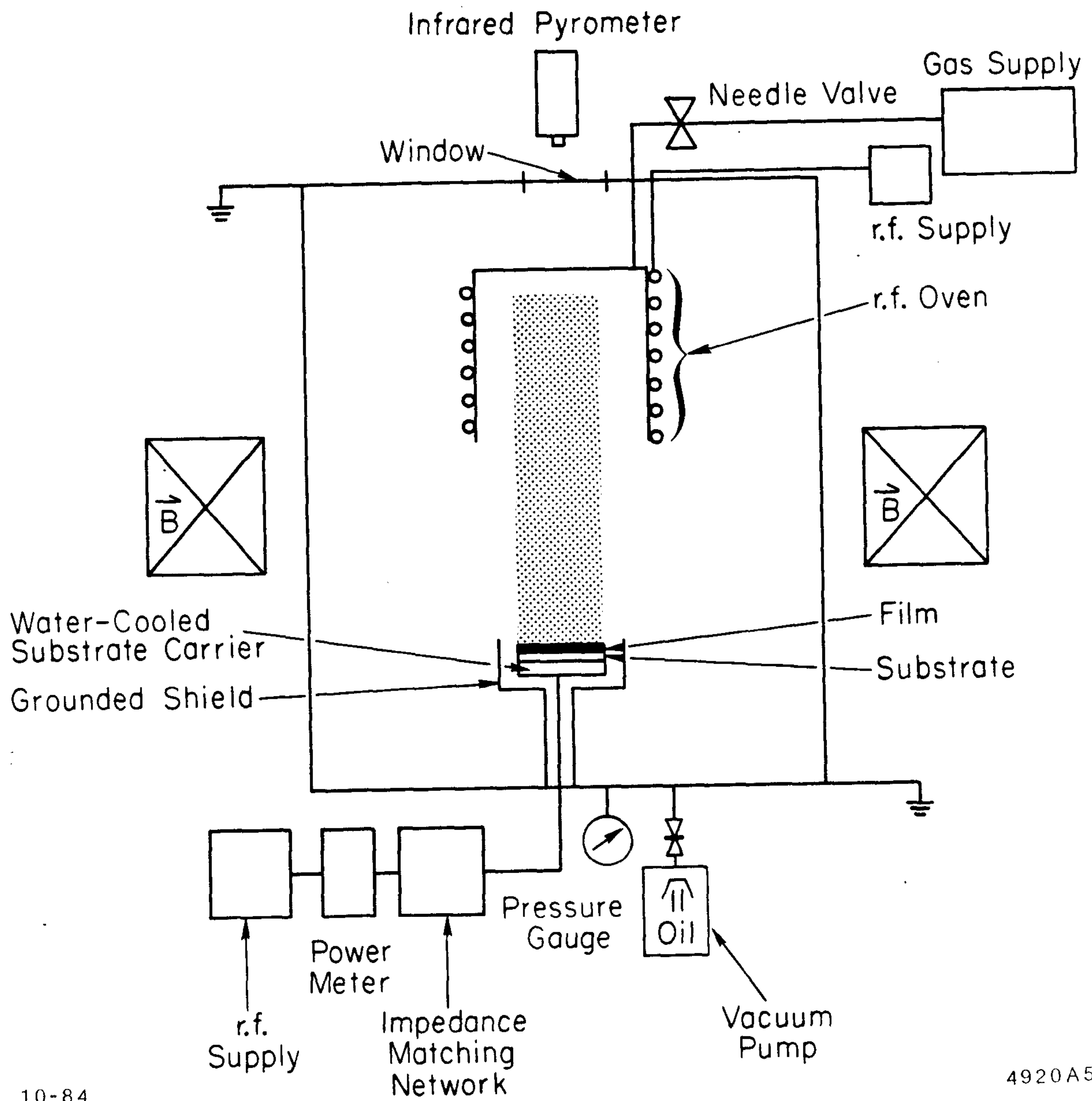

Fig. 1

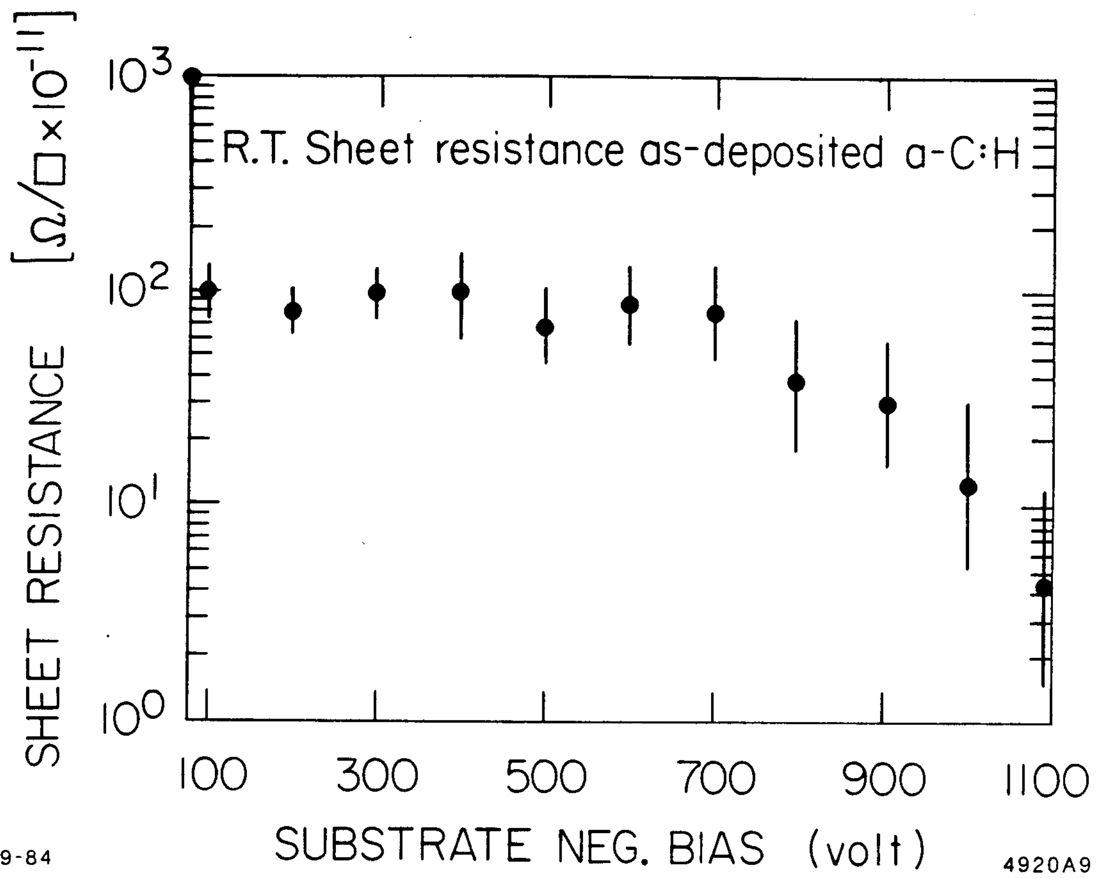

Fig. 2

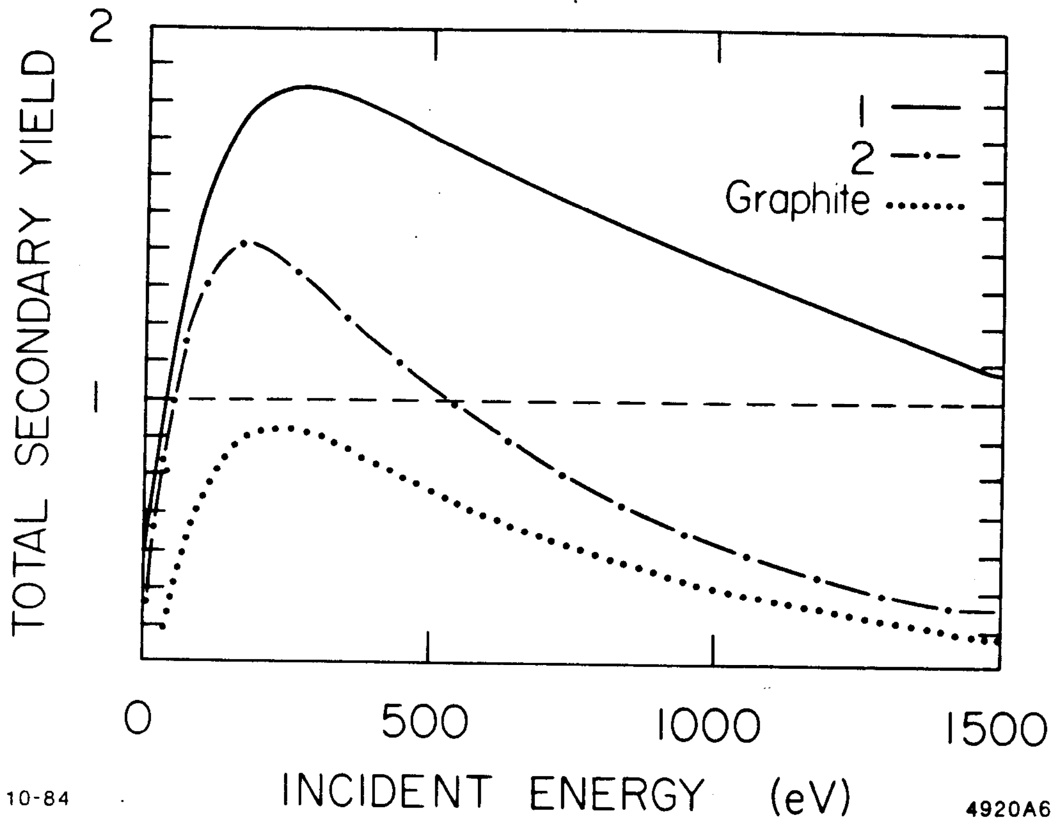

Fig. 3

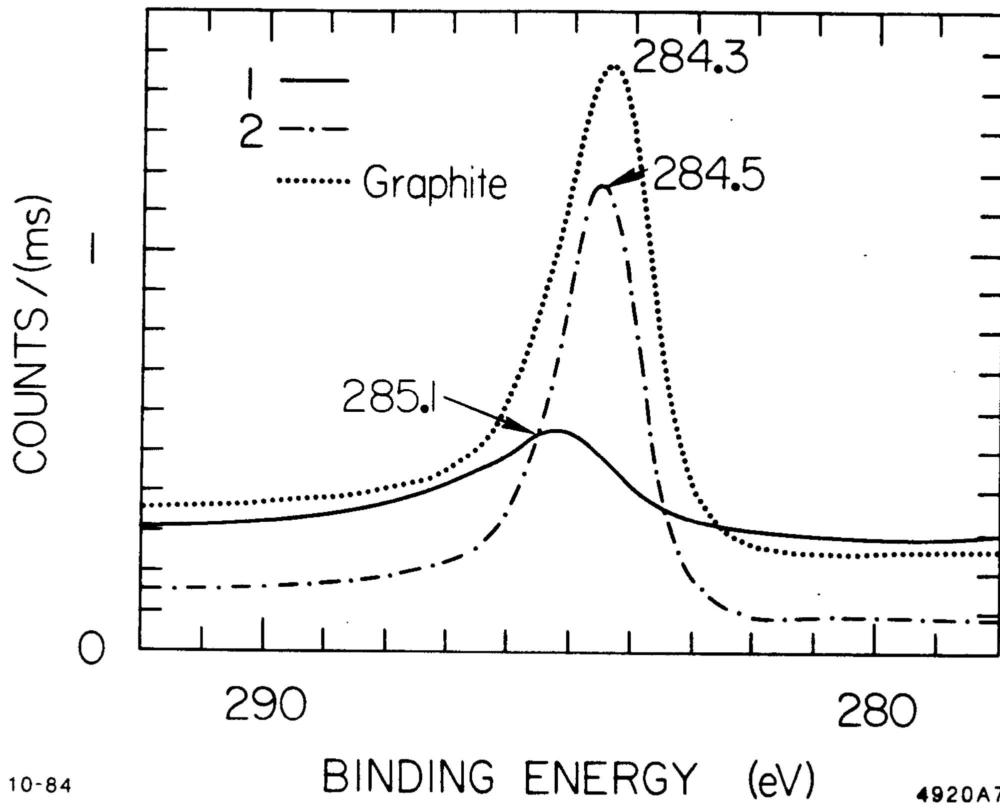

Fig. 4

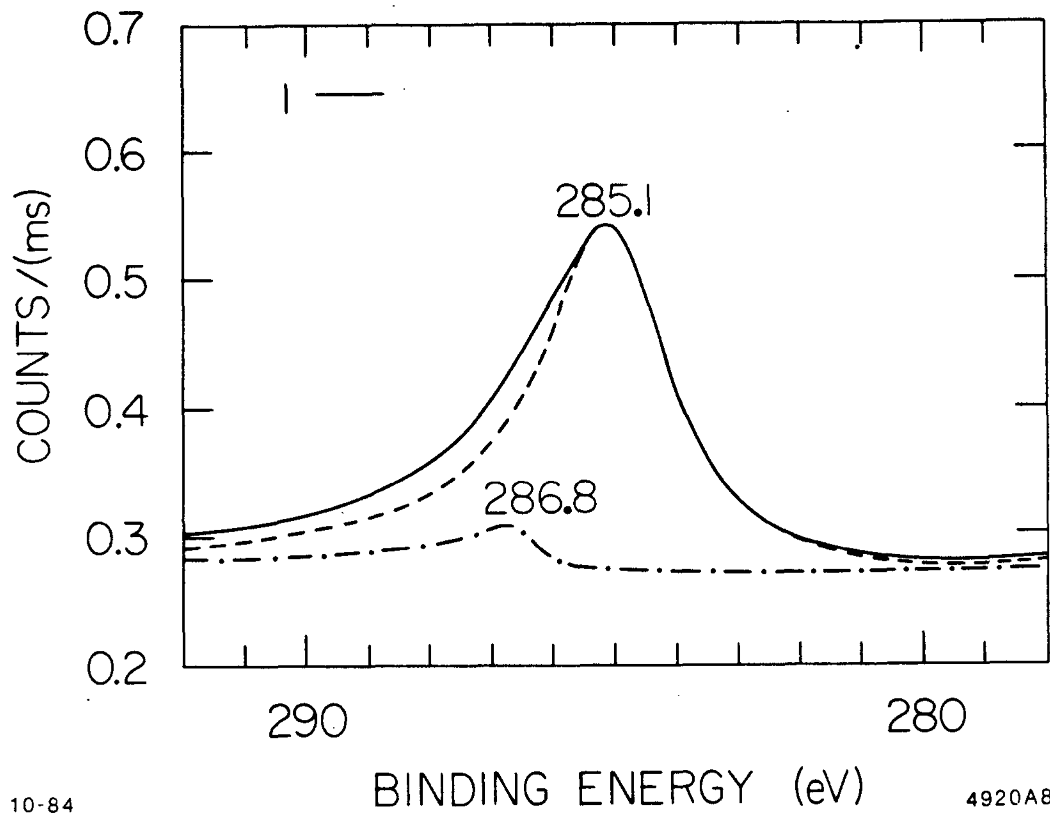

Fig. 5

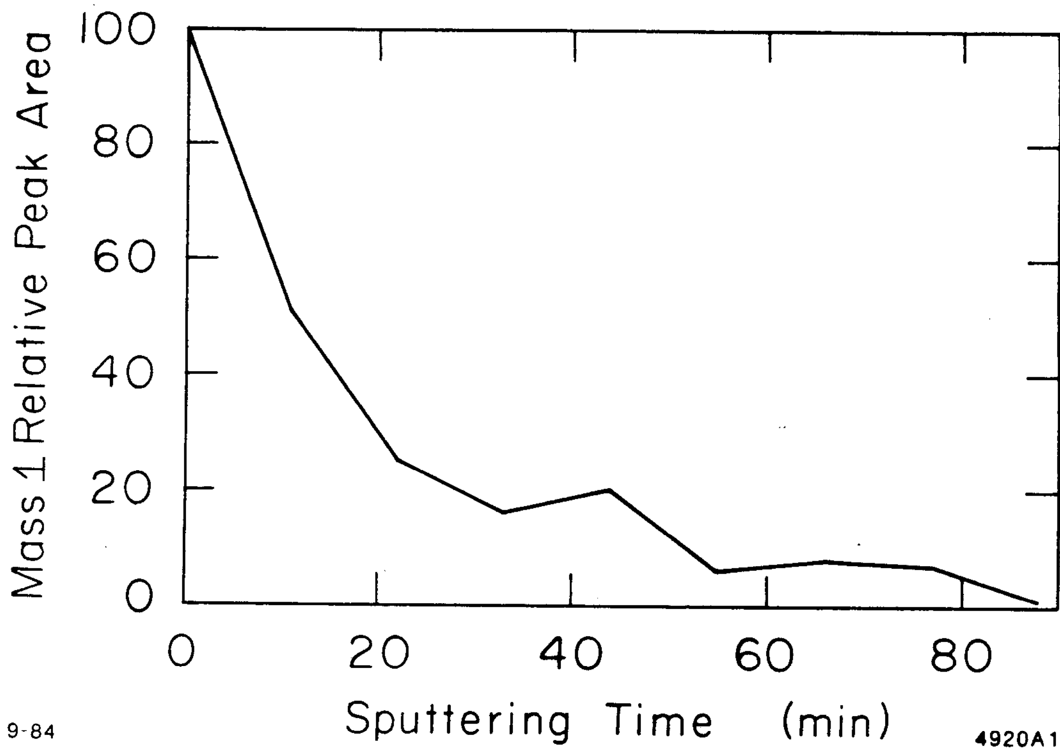

Fig. 6